# Journal of Materials Chemistry C

Accepted Manuscript


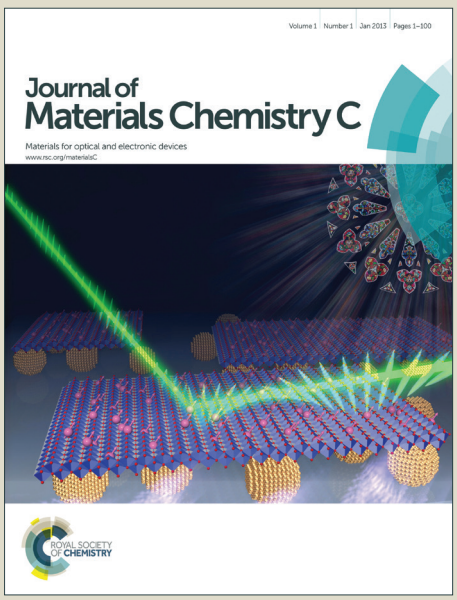





ROYAL SOCIETY OF CHEMISTRY

www.rsc.org/materialsC

# Enhancing photovoltaic properties of terpolymers containing benzo[1,2-*b*:4,5-*b'*]dithiophene, phenanthro[4,5-*abc*]phenazine and benzo[*c*][1,2,5]thiadiazole with a changing substituents

Qunping Fan [a], Yu Liu [a,*], Manjun Xiao [a], Wenyan Su [a], Huishan Gao [a], Jianhua Chen [a], Hua Tan [a], Yafei Wang [a], Renqiang Yang [b,*], Weiguo Zhu [a,*]

[a] *College of Chemistry, Xiangtan University, Key Lab of Environment-Friendly Chemistry and Application in Ministry of Education, Xiangtan 411105, China*

[b] *Qingdao Institute of Bioenergy and Bioprocess Technology, Chinese Academy of Sciences, Qingdao 266101, China*

Corresponding author: Prof. Yu Liu; Renqiang Yang; Weiguo Zhu

Tel: +86-731-58293377

Fax: +86-731-58292251

E-mail addresses: liuyu03b@126.com; yangrq@qibebt.ac.cn; zhuwg18@126.com

**Abstract**: In this work, three novel donor-acceptor (D-A)-type random conjugated terpolymers of PBDTT-PPzBT-H, PBDTT-PPzBT-F and PBDTT-PPzBT-O were synthesized by copolymerizing electron-rich 5,8-dialkylthienyl substituted benzo[1,2-*b*:4,5-*b*′]dithiophene (BDTT) and two electron-deficient phenanthro-[4,5-*abc*]phenazine (PPz) and benzo[*c*][1,2,5]thiadiazole (BT) units. By changing the substituents at 5,6-positions of BT, the optoelectronic properties of the terpolymers could be rationally adjusted for application as donor materials in polymer solar cells (PSCs). As a result, these terpolymers exhibited different light absorption properties, HOMO energy levels and hole mobilities, which contributed to the optimization of short-circuit current ($J_{sc}$), open-circuit voltage ($V_{oc}$) and fill factor (*FF*) properties, respectively. Pleasingly, a maximum power conversion efficiency (PCE) of 6.3% was obtained with an $V_{oc}$ of 0.75 V, a $J_{sc}$ of 13.0 mA cm$^{-2}$ and a *FF* of 64.8% in the PBDTT-PPzBT-O based PSCs using [6,6]-phenyl-$C_{71}$-butyric acid methyl ester ($PC_{71}BM$) as an acceptor, while PBDTT-PPzBT-H and PBDTT-PPzBT-F based devices also demonstrated a PCE of more than 4.5%. To the best of our knowledge, these are the highest recorded maximum PCE, $J_{sc}$ and *FF* values obtained to date compared with previously reported phenazine copolymeric derivatives in BHJ-PSCs. This work illustrated the potential of these random conjugated terpolymers as promising donor materials in the application of PSCs.

**Keywords:** Bulk heterojunction; Polymer solar cells; Benzo[1,2-*b*:4,5-*b*′]dithiophene; Phenanthro[4,5-*abc*]phenazine; Benzo[*c*][1,2,5]thiadiazole; Terpolymer

## 1. Introduction

All over the world, increasing demand for energy has become a serious problem. As a result, bulk heterojunction (BHJ) polymer solar cells (PSCs) have attracted considerable attention as promising renewable energy resources due to their low cost, light weight, applications in flexible and large-area devices.[1-3] In order to improve the photovoltaic performance of PSCs, tremendous efforts have been devoted to the development of new solution processable conjugated polymer donor materials containing electron-rich units (donor, D) and electron-deficient units (acceptor, A) with broad absorption spectra and high absorption coefficients in visible-ultraviolet region resulting from intramolecular charge transfer (ICT) interaction.[4-10] Recently, a major breakthrough was made in enhance of power conversion efficiencies (PCE) due to the development of novel conjugated polymers.[11-14] For example, a record PCE of up to 10.8% had been harvested in PSCs.[11]

Optimized photovoltaic properties in polymer donor material can offer high short-circuit current density ($J_{sc}$), open-circuit voltage ($V_{oc}$), fill factor (*FF*) and result in a high PCE from PSCs.[15-17] Unfortunately, most D-A alternating polymers are unable to obtain high PCE due to the imbalance between $J_{sc}$ and $V_{oc}$.[18,19] In this regard, terpolymers composed of three different units in the polymer backbone are promising candidates as they can exhibit the synergetic effects of each unit by tuning the composition ratio, thus demonstrating broad absorption, a deep highest occupied molecular orbital (HOMO) energy level, high charge mobility and good solubility.[20-29] For instance, Jo *et al.* obtained a class of random conjugated terpolymers by tuning

the composition ratio of diketopyrrolopyrrole (DPP) and isoindigo as co-electron accepting units in D-A-type polymers.[21] This kind of terpolymer provided a suitable balance between light absorption and the photon flux of the solar spectrum and a PCE of 6.04% with a $V_{oc}$ of 0.77 V, $J_{sc}$ of 13.52 mA $cm^{-2}$ and *FF* of 58.0% was obtained in the polymers based on BHJ-PSCs. Wei *et al.* exhibited another class of terpolymers with a D-A-type alternating backbone of benzodithiophene (BDT)-benzooxadiazole-DPP by tuning the composition ratio of two co-electron accepting units.[22] Similar to other analogues,[23-25] a maximum PCE of 6.8% with a $V_{oc}$ of 0.73 V, $J_{sc}$ of 17.0 mA $cm^{-2}$ and *FF* of 55.0% was achieved in the polymers based on PSCs. Recently, phenazine derivatives as acceptor units have shown promising properties for application in PSCs, due to their relatively large π-conjugated system with planar structure that is favorable for strong intermolecular π-π stacking and its self-assembled characteristics, thus benefiting charge transportation and absorption in long wavelengths.[30-33] For instance, Jen *et al.* reported a polymer of PIDT-phanQ with an alternating D-A backbone of indacenodithiophene (IDT) and phenanthrene-qunioxaline (phanQ), a maximum PCE of 6.24% with a hole mobility ($\mu_h$) of 0.024 $cm^2\ V^{-1}\ s^{-1}$ that was obtained in PIDT-phanQ based PSCs.[30] Our group also reported a polymer of PTTPPz-BDTT with the phenanthro[4,5-*abc*]phenazine (PPz) acceptor unit and a maximum PCE of 4.87% with a *FF* of 62.5%.[31]

In addition, another type of polymers with 7,8-dialkylthienyl benzo[1,2-*b*:4,5-*b*′]dithiophene (BDTT) units was utilized as an donor materials for application in PSCs, due to its relatively large and planar conjugated structure, and

was favorable for π-π stacking, improvement of carrier transportation and light absorption.[34-36] For example, a maximum PCE of 9.48% with a $J_{sc}$ of 17.46 mA cm$^{-2}$ and $\mu_h$ of 0.01 cm$^2$ V$^{-1}$ s$^{-1}$ was obtained from PBDT-TS1 based PSCs by Hou group.[34] Furthermore, some benzo[*c*][1,2,5]thiadiazole (BT) derivatives as acceptor units have been widely used with D-A-type polymers for application in PSCs, due to their strong electron-accepting ability and 5,6-positions substituted properties.[37-42] Woo *et al.* reported a polymer of PTBT14 with a 5,6-dialkoxy substituted BT-O as acceptor unit, and a maximum PCE of 5.56% with a $\mu_h$ of 0.02 cm$^2$ V$^{-1}$ s$^{-1}$ was achieved in the PTBT14 based PSCs.[39] Watkins *et al.* reported a polymer of BFS4 with a 5,6-difluoro substituted BT-F as acceptor unit, and a maximum PCE of 7.80% with a $V_{oc}$ of 0.90 V, $J_{sc}$ of 14.2 mA cm$^{-2}$ and *FF* of 61.1% was obtained in the BFS4 based PSCs.[41]

Inspired by the aforementioned works, the synthesis and optical and electrochemical characterization of three novel D-A-type random conjugated terpolymers is reported herein, in addition to their photovoltaic performances in PSCs. Their molecular structures are shown in Scheme 1. It was expected that the construction of the BDTT-PPzBT backbone and changes to the substituents at 5,6-positions of BT unit would enhance intramolecular ICT interaction and intermolecular π-π stacking, thereby broadening the absorption spectrum, reducing the HOMO energy level, increasing the hole mobility and improving the photovoltaic properties of the resulting terpolymers. As expected, the PSC based on PBDTT-PPzBT-O/$PC_{71}BM$ exhibited the best performance with a PCE of 6.3%, $V_{oc}$ of 0.75 V, $J_{sc}$ of 13.0 mA cm$^{-2}$ and *FF* of 64.8%. This suggested that changing the

substituents at the 5,6-positions of BT unit provides potential for application in organic solar cells. Future work will focus on tuning the energy levels of the terpolymers to achieve enhanced photovoltaic performance.

## 2. Experimental section

*2.1. Instrumentations and characterization*

The molecular weights were determined using a Waters GPC 2410 in tetrahydro-furan via a calibration curve of polystyrene as standard. Thermo gravimetric analyses (TGA) were conducted under a dry nitrogen gas flow at a heating rate of 20 $^{\circ}$C min$^{-1}$ on a Perkin-Elmer TGA 7. Differential scan calorimetry (DSC) measurements were carried out with a Netzsch DSC-204 under nitrogen flow at heating and cooling rates of 10 $^{\circ}$C min$^{-1}$. UV-Vis absorption spectra were recorded on a HP-8453 UV visible system. Cyclic voltammograms (CV) were carried out on a CHI660A electrochemical work station with a three electrode electrochemical cell in a 0.1 M tetrabutylammonium hexafluorophosphate ($TBAPF_6$) acetonitrile solution with a scan100 mV s$^{-1}$ at room temperature under argon atmosphere. In this three-electrode cell, a platinum rod, platinum wire and Ag/AgCl electrode were used as a working electrode, counter electrode and reference electrode, which was calibrated against the redox potential of ferrocene/ferrocenium ($Fc/Fc^{+}$). Surface morphologies were recorded by atomic force microscopy (AFM) on a Veeco-134 DI multimode NS-3D apparatus in a tapping mode under normal air condition at room temperature.

*2.2. Fabrication and characterization of polymer solar cells*

The PSCs were fabricated using indium tin oxide (ITO) glass as an anode, Ca/Al as

a cathode, and a blend film of the polymer/PCBM as a photosensitive layer. After a 30 nm buffer layer of poly-(3,4-ethylenedioxy-thiophene) and polystyrene sulfonic acid (PEDOT:PSS) was spin-coated onto the precleaned ITO substrate, the photosensitive layer was subsequently prepared by spin-coating a solution of the polymer/$PC_{71}BM$ (1:2, *w/w*) in 1,2-dichlorobenzene (ODCB) on the PEDOT:PSS layer with a typical concentration of 15 (or 30) mg $mL^{-1}$, followed by annealing at 80 $^{\circ}C$ for 10 minutes to remove ODCB. Ca (10 nm) and Al (100 nm) were successively deposited on the photosensitive layer in vacuum and used as top electrodes. The current-voltage (I-V) characterization of the devices was carried out on a computer-controlled Keithley source measurement system. A solar simulator was used as the light source and the light intensity was monitored by a standard Si solar cell. The active area was $7\times10^{-2}$ $cm^2$ for each cell. The thicknesses of the spun-cast films were recorded by a profilometer (Alpha-Step 200, Tencor Instruments). The external quantum efficiency (*EQE*) was measured with a Stanford Research Systems model SR830 DSP lock-in amplifier coupled with WDG3 monochromator and a 150 W xenon lamp.

*2.3. Materials*

2,5-bis(trimethytin)-7,8-bis(5-(2-ethylhexyl)thiophen-2-yl)benzo[1,2-*b*:4,5-*b*′]dithiophene (M1), 4,7-bis(5-bromo-4-hexylthiophen-2-yl)benzo[*c*][1,2,5]thiadiazole (M3), 4,7-bis(5-bromo-4-octylthiophen-2-yl)-5,6-difluorobenzo[*c*][1,2,5]thiadiazole (M4) and 4,7-bis(5-bromothiophen-2-yl)-5,6-dioctyloxybenzo[*c*][1,2,5]thiadiazole (M5) were purchased directly from the Suna Tech Inc. The other reagents and chemicals were purchased from commercial sources (Aldrich, TCI) and used without further

purification unless stated otherwise. The monomer 10,13-bis(5-bromothiophen-2-yl)-11,12-bis(octyloxy)phenanthro[4,5-*abc*]phenazine (M2) was prepared according to literature procedures.[31] The detailed syntheses of these terpolymers were presented following the procedures described herein.

*2.4. Synthesis of terpolymers*

*2.4.1. Synthesis of terpolymer PBDTT-PPzBT-H*

In a dry 25 mL flask, tris(dibenzylideneacetone)dipalladium(0) ($Pd_2(dba)_3$, 5.0 mg) and tri(*o*-tolyl)phosphine (P(*o*-Tol)$_3$, 10.0 mg) were added to a solution of M1 (118 mg, 0.13mmol), M2 (57 mg, 0.065mmol) and M3 (41 mg, 0.065mmol) in 8 mL degassed toluene under nitrogen and stirred vigorously at 100 °C for 0.5 h until the reaction system becomes a viscous state. After cooled to room temperature, the mixture was poured into acetone (100 mL) and the precipitation was occurred. It was collected by filtration and Soxhlet-extracted successively with hexane, acetone and diethyl ether each for 12 h. Then the solvent was changed to be chloroform ($CHCl_3$). After that the still remained solid was dissolved with ODCB (100 mL) and precipitated with methanol to get the dark solid (127 mg, 83.6%). Anal. Calcd for $C_{140}H_{158}N_4O_2S_{13}$: C, 71.69; H, 6.79; N, 2.39; S, 17.77. Found: C, 71.00; H, 7.30; N, 2.38; S, 18.67.

*2.4.2. Synthesis of terpolymer PBDTT-PPzBT-F*

PBDTT-PPzBT-F was prepared according to the synthetic procedure of PBDTT-PPzBT-H by the reaction among M1 (118 mg, 0.13mmol), M2 (57 mg, 0.065mmol), M4 (47 mg, 0.065mmol), $Pd_2(dba)_3$ (5.0 mg) and P(o-Tol)$_3$ (10.0 mg) in

dry toluene (8 mL). The reaction was stirred for 0.5 h until the reaction system becomes a viscous state and the terpolymer was collected as a dark solid (129 mg, 81.6%). Anal. Calcd for $C_{144}H_{164}F_2N_4O_2S_{13}$: C, 70.95; H, 6.87; N, 2.30; S, 17.10. Found: C, 70.34; H, 7.69; N, 2.29; S, 18.31.

*2.4.3. Synthesis of terpolymer PBDTT-PPzBT-O*

PBDTT-PPzBT-O was prepared according to the synthetic procedure of PBDTT-PPzBT-H by the reaction among M1 (117 mg, 0.13mmol), M2 (57 mg, 0.065mmol), M5 (46 mg, 0.065mmol), $Pd_2(dba)_3$ (5.0 mg) and P(o-Tol)$_3$ (10.0 mg) in dry toluene (8 mL). The reaction was stirred for 0.5 h until the reaction system becomes a viscous state and the terpolymer was collected as a dark solid (141 mg, 89.2%). Anal. Calcd for $C_{144}H_{166}N_4O_4S_{13}$: C, 71.07; H, 6.87; N, 2.30; S, 17.07. Found: C, 71.08; H, 7.76; N, 2.33; S, 18.43.

## 3. Results and discussion

*3.1. Synthesis and thermal properties*

The synthetic routes of three terpolymers of PBDTT-PPzBT-H, PBDTT-PPzBT-F and PBDTT-PPzBT-O are outlined in Scheme 2. All the terpolymers were synthesized at 100 $^{\circ}$C for 0.5 h by the palladium-catalyzed Stille-coupling polymerization with moderate yield. The actual molecular composition of these terpolymers was determined by the elemental analysis. The results showed that M1/M2/M3 (M4 or M5) ratio was 2/1/1 in these terpolymers, and consistent with the molar feed ratio of M1/M2/M3 (M4 or M5). The molecular weight of these terpolymers were determined by GPC relative to polystyrene standards and the related data are listed in Table 1. The

number average molecular weights ($M_n$) are observed to be 29 kDa for PBDTT-PPzBT-H, 45 kDa for PBDTT-PPzBT-F, and 52 kDa for PBDTT-PPzBT-O, respectively. Although the molar mass of the synthesized terpolymers shows differences, but these terpolymers exhibit similar solubility, and can be found only slightly soluble in most of the organic solvents such as $CHCl_3$, tetrahydrofuran (THF), chlorobenzene (CB) and ODCB at room temperature. The poor solubility of these terpolymers may be caused by the large planar polymer backbone, which induced stronger intermolecular interactions.[31-33]

The recorded TGA curves of these random terpolymers are depicted in Fig. 1, and the corresponding data summarized in Table 1. The thermal decomposition temperatures ($T_d$) are observed to be 350 °C for PBDTT-PPzBT-H, 363 °C for PBDTT-PPzBT-F and 341 °C for PBDTT-PPzBT-O at 5% weight loss, respectively. Compared to the PBDTT-PPzBT-H, PBDTT-PPzBT-F exhibits a increased $T_d$ value and PBDTT-PPzBT-O exhibits a decreased $T_d$ value, which means that two fluorine atom (or two octyloxy groups) at 5,6-positions of BT play a positive (or negative) role in increasing thermal stability of its polymer. Moreover, no thermal transition pointis observed from 50 °C to 180 °C in the DSC curves (Fig. S1), indicating that these terpolymers have amorphous characteristics.[43]

*3.2. Optical properties*

Fig. 2a and 2b show the normalized UV-Vis absorption spectra of these terpolymers in ODCB solution with a concentration of $1 \times 10^{-5}$ M and neat film. The detailed parameters are summarized in Table 2. In a solution state, all of the terpolymers

exhibited a similar UV-Vis spectra with two absorption bands, among which the high-lying absorption band from 340 to 500 nm was assigned to the π-π* transition and another low-lying absorption band from 500 to 800 nm was attributed to the strong photoinduced ICT effect from the BDTT donor unit to the PPz and BT aceptor units. Interestingly, the three terpolymers showed similar absorption profiles with a slight shift in ODCB solution (Fig. 2a). Generally, the absorption spectra of polymers move to longer wavelength region by introduction of electron donating units (O>H>F), but there, appending two octylloxy groups at 5,6-positions of BT make the corresponding terpolymer PBDTT-PPzBT-O present a blue-shift absorption spectrum. Therefore, alkyloxy groups appended at BT unit do not always broaden the absorption spectrum for its copolymers although alkyloxy group is a common electron-donating group. Similar reports were observed in another dioctyloxy side chains substituted D-A polymers.[12] Compared with the absorption spectra in ODCB solution, these terpolymers in neat films displayed an additional shoulder peak at 658, 602 and 596 nm in addition to the red-shift high energy peak of 618, 649 and 626 nm for PBDTT-PPzBT-H, PBDTT-PPzBT-F and PBDTT-PPzBT-O (Fig. 2b), respectively, implying that all of these terpolymers possessed strong intermolecular packing potential in a solid state. Furthermore, PBDTT-PPzBT-F exhibited the largest red-shift absorption about 45 nm, which was ascribed to the fluorine atom substituent effect strengthen the intermolecular packing potential,[44] while the other two terpolymers displayed some red-shift in the thin films. Based on the onset of the film absorption, the optical band gaps ($E_g^{opt}$) of PBDTT-PPzBT-H, PBDTT-PPzBT-F and

PBDTT-PPzBT-O were calculated as 1.61, 1.56 and 1.63 eV, respectively. The extended absorption edge in the long wavelength region was attributed to the more aggregated configuration formed in a solid state. Fig. 2c shows the UV-Vis absorption spectra of the terpolymer/$PC_{71}BM$ blend films at the optimized ratio of 1/2 (*w/w*). The increasing the absorption intensities were observed in PBDTT-PPzBT-H, PBDTT-PPzBT-F and PBDTT-PPzBT-O blend films. This suggested that the two fluorine atoms or octyloxy groups were available instead of the two hydrogen atoms at the 5,6-positions of BT in order to enhance the UV-Vis absorption ability for the terpolymers.

*3.3. Electrochemical properties*

The electrochemical properties of the terpolymers were investigated through cyclic voltammetry (CV). Fig. 3 shows the recorded CV curves of the terpolymers using an Ag/AgCl electrode as a reference and the redox potential of ferrocene/ferrocenium ($Fc/Fc^+$) as a calibrated standard. The relevant data are summarized in Table 2. The observed onset oxidation potentials ($E_{ox}$) for PBDTT-PPzBT-H, PBDTT-PPzBT-F and PBDTT-PPzBT-O were 0.80 V, 0.97 and 0.95 V, respectively. The HOMO energy levels of terpolymers were calculated according to the empirical equation:[45] $E_{HOMO}$= - ($E_{ox}$ - 0.45) - 4.8 eV. As a result, the HOMO energy levels ($E_{HOMO}$) were estimated at -5.15 eV for PBDTT-PPzBT-H, -5.32 eV for PBDTT-PPzBT-F and -5.30 eV for PBDTT-PPzBT-O, respectively. The LUMO energy levels ($E_{LUMO}$) levels of the terpolymers were calculated by "$E_{LUMO}$ = $E_{HOMO}$ + $E_g^{opt}$". Compared to PBDTT-PPzBT-H, PBDTT-PPzBT-F and

PBDTT-PPzBT-O presented a significant decrease in $E_{HOMO}$ levels due to the hydrogen bonding effects.[39-41] As known, $V_{oc}$ of BHJ-PSCs is directly proportional to the offset between the HOMO level of the donor and LUMO level of the acceptor. It could thus be concluded that the structures of fluorine atoms or alkoxy groups substituted could improve the $V_{oc}$.

The HOMO and LUMO distributions of polymers were calculated by density functional theory (DFT) (B3LYP; 6-31G*) method. As shown in Fig. 4, these terpolymers showed similar electron-state-density distributions of the HOMO, while two fluorine atoms or two octyloxyl groups at 5,6-positions of BT instead of two hydrogen atoms slightly decreased the HOMO of these terpolymers, and consistent with the CV measurements. It is worth noting that the electron-state-density distributions of the LUMO are mostly located on the acceptor units of BT (or BT-F or BT-O), which means that the electron withdrawing ability of BT (or BT-F or BT-O) unit is stronger than PPz unit. The DFT calculation results showed that BT (or BT-F or BT-O) gives the major influence to LUMO energy level of the terpolymers with the two electron-withdrawing units. These results are consistent with the DFT calculation results of those BDTT-*alt*-DTPPz and BDTT-*alt*-DTBT copolymers (see Fig. S2).

*3.4. Hole mobility*

To further understand the effect of chemical structures on the photovoltaic performance of terpolymers in PSC devices, the hole mobilities ($\mu_h$) of these photoactive layers were measured by the space charge limited current (SCLC) method in the hole devices with a structure of ITO/PEDOT:PSS/terpolymer:$PC_{71}BM$/Au at

the optimized conditions. The SCLC could be estimated using the Mott-Gurney equation: $J = (9/8)\varepsilon_0\varepsilon_r\mu_h(V/L^3)$,[46] where, $J$ is current density, $\varepsilon_r$ is dielectric constant of terpolymer, $\varepsilon_0$ is free-space permittivity ($8.85 \times 10^{-12}$ F/m), $d$ is thickness of the blended film layer, $V = V_{appl} - V_{bi}$, $V$ is the effective voltage, $V_{appl}$ is applied voltage, and $V_{bi}$ is built-in voltage that results from the work function difference between the anode and cathode. Fig. 5 displays the *J-V* curves of these hole devices containing terpolymer/$PC_{71}BM$ active layers, respectively. As summarized in Table 3, the hole mobilities of PBDTT-PPzBT-H, PBDTT-PPzBT-F and PBDTT-PPzBT-O were calculated as $4.64 \times 10^{-5}$, $8.61 \times 10^{-5}$ and $3.75 \times 10^{-4}$ $cm^2 V^{-1} s^{-1}$ in the hole terpolymer/ $PC_{71}BM$-based devices, respectively. Compared with the previously reported binary polymer PTTPz-BDTT based on PPz and BDTT units,[31] significantly increased mobility was achieved for PBDTT-PPzBT-O. This suggested that incorporating BT with two octyloxy substitutents into a terpolymer facilitated increased hole mobility, which could be ascribed to enhanced interchain π-π interactions.[39] Obviously, high hole mobility for PBDTT-PPzBT-O was responsible for the high *FF* level and PCE in the devices.

*3.5. Photovoltaic properties*

To investigate the photovoltaic properties of the terpolymers, BHJ-PSCs were also fabricated with a general device structure of ITO/PEDOT:PSS/active layer/Ca/Al. The active layer (D/A, terpolymer/$PC_{71}BM$) was obtained from an ODCB solution at different concentrations (30 mg/mL for PBDTT-PPzBT-H and PBDTT-PPzBT-F, 15 mg/mL for PBDTT-PPzBT-O). As known, the photovoltaic performances of PSCs are

strongly affected by the processing parameters, including the D/A ratio (*w/w*), annealing temperature and spin-coating rate.[31] Optimized parameters were obtained and Fig. S3, S4 and S5 depict the *J-V* characteristics of terpolymer/$PC_{71}BM$-based devices at different ratios, annealing temperatures and spin-coating rates, respectively. The resulting photovoltaic data are summarized in Tables S1, S2 and S3, respectively. The terpolymer/$PC_{71}BM$-based PSCs have an optimized D/A ratio of 1:2 and annealing temperature of 80 $^{\circ}$C, while different spin-coating rates were utilized for the devices (3000 rpm for PBDTT-PPzBT-H, 2500 rpm for PBDTT-PPzBT-F, 1000 rpm for PBDTT-PPzBT-O), respectively. As shown in Fig. 6, the typical devices exhibited typical *J-V* characteristics under these optimized conditions. Device parameters, such as $J_{sc}$, $V_{oc}$, *FF* and PCE, were deduced from the *J-V* characteristics and are summarized in Table 3. All of the three typical devices exhibited excellent photovoltaic properties, in which PCE was more than 4.5% and $J_{sc}$ more than 12.0 mA $cm^{-2}$.

As shown in Fig. 6, the PBDTT-PPzBT-F/$PC_{71}BM$ and PBDTT-PPzBT-O/$PC_{71}BM$-based devices exhibited better photovoltaic properties compared with the PBDTT-PPzBT-H/$PC_{71}BM$-based device, which could be attributed to the two fluorine atoms and octyloxy units substituting BT in the terpolymers, causing significant increases in the $V_{oc}$ (from 0.67 V to 0.74 V and 0.75 V) and *FF* (from 55.0% to 59.6% and 64.8%) at their PSCs. Furthermore, compared with the PBDTT-PPzBT-F/$PC_{71}BM$-based device, the PBDTT-PPzBT-O/$PC_{71}BM$-based device showed a significant increase in the *FF* from 59.6% to 64.8%. High *FF* value was

responsible for the high hole mobility of the PBDTT-PPzBT-O based hole devices. Natably, compared to the previous alternating M1-*alt*-M2 polymer PTTPPz-BDTT (PCE of 4.86% with a $V_{oc}$ of 0.70 V, $J_{sc}$ of 11.1 mA cm$^{-2}$ and *FF* of 62.5%),[31] PBDTT-PPzBT-F and PBDTT-PPzBT-O exhibit high $V_{oc}$, $J_{sc}$ and PCE values, which was attributed the introduction of the second receptor units of M4 or M5 in the terpolymer systems reduced the HOMO levels and promoted the photonic response of these terpolymers. As a result, a maximal PCE of up to 6.3% was obtained with $V_{oc}$ of 0.75 V, $J_{sc}$ of 13.0 mA cm$^{-2}$ and *FF* of 64.8% in the PBDTT-PPzBT-O/$PC_{71}BM$-based device. To the best of our knowledge, these were the highest PCE, $J_{sc}$ and *FF* values recorded to date as compared with previously reported phenazine copolymeric derivatives in BHJ-PSCs.[30-33] This was attributed to the introduction of two octyloxy substituted BT.

In order to understand why the PBDTT-PPzBT-O/$PC_{71}BM$-based devices displayed the highest PCE values, the external quantum efficiency (*EQE*) curves of devices under the optimized conditions were also measured. As depicted in Fig. 7, all of the terpolymers/$PC_{71}BM$-based devices demonstrated a very efficient photo-response in a broad range from 310 to 750 nm, corresponding to the high *EQE* of over 40% obtained in a broad range from 340 to 670 nm for all three devices. Maximum *EQE*s were obtained in the terpolymers/$PC_{71}BM$-based devices of 72% at 424 nm for PBDTT-PPzBT-H, 79% at 411 nm forPBDTT-PPzBT-F and 83% at 400 nm for PBDTT-PPzBT-O, respectively. Obviously, the PBDTT-PPzBT-O based device showed a higher *EQE* in a range from 350 to 650 nm compared with the

PBDTT-PPzBT-H and PBDTT-PPzBT-F based devices. Higher *EQE* values and more intense absorptions (see Fig. 2c) powerfully facilitated the PBDTT-PPzBT-O based devices to provide higher $J_{sc}$ values. Meanwhile, in accordance with the *EQE* curves and the solar irradiation spectrum, the integral $J_{sc}$ values were determined as 12.0, 12.2 and 12.6 mA $cm^{-2}$ for the PBDTT-PPzBT-H, PBDTT-PPzBT-F and PBDTT-PPzBT-O based devices, respectively, which were in agreement with the measured $J_{sc}$ values within a 4% error margin.

*3.6. Film morphology*

The morphology of the blend films under the optimized conditions could also explain the enhanced photovoltaic performance of the PBDTT-PPzBT-O based device. Fig. 8 displays the surface morphology of the terpolymers/$PC_{71}BM$ blend films recorded by atomic force microscopy (AFM) in a surface area of 5 × 5 $\mu m^2$ using the tapping mode. The root mean square (RMS) roughness from the height images were determined as 1.30, 1.26 and 0.91 nm for the PBDTT-PPzBT-H, PBDTT-PPzBT-F and PBDTT-PPzBT-O based blend films, respectively. A smoother surface was observed for the PBDTT-PPzBT-O based blend film. Therefore, higher $J_{sc}$ and PCE values for the PBDTT-PPzBT-O based device were ascribed to more efficient charge transport properties and smoother morphology, in addition to better absorption properties, which provided a *FF* of 64.8% and better device performance with a PCE of up to 6.3%.

*3.7. XRD analysis*

The XRD patterns of these terpolymers were carried out in order to investigate the molecular interactions in details and shown in Fig. 9. It is observed that PBDTT-PPzBT-H, PBDTT-PPzBT-F and PBDTT-PPzBT-O show a strong peak at $2\theta$ = 22.1°, $2\theta$ = 22.9° and $2\theta$ = 22.7°, respectively, indicating that all polymers have effective π-π stacking, due to the great aggregation of PPz unit.[31] Compared with PBDTT-PPzBT-H, PBDTT-PPzBT-F and PBDTT-PPzBT-O exhibited increasing $2\theta$ peak. It implies that incorporating the fluorine atom or octyloxy side chain substituents at 5,6-positions of BT would enhance intermolecular π-π stacking. It is consistent with the results of AFM and charge carrier mobility measurements. Based on the above investigation shown that large planar PPz unit and 5,6-difluorine or 5,6-dioctyloxy substituted BT unit favors to provide effective π-π stacking of polymers, which is in favor of exciton dissociation and charge transportation, offering largely higher $J_{sc}$ and *FF* in the resulting devices.[31,40]

## 4. Conclusions

In this work, three novel $A_1$-D-$A_2$ terpolymers of PBDTT-PPzBT-H, PBDTT-PPzBT-F and PBDTT-PPzBT-O were synthesized by copolymerizing electron-rich BDTT and two electron-deficient PPz and BT units. By changing the substituents at 5,6-positions of BT, the photophysical, electrochemical and charge transport properties of the terpolymers could be rationally adjusted. A maximum PCE of 6.3% with an $V_{oc}$ of 0.75 V, $J_{sc}$ of 13.0 mA cm$^{-2}$ and *FF* of 64.8% was exhibited in the PBDTT-PPzBT-O/$PC_{71}BM$ based PSCs. The other terpolymer based devices also demonstrated PCEs of more than 4.5%. To the best of our knowledge, these were the

highest recorded PCE, $J_{sc}$ and *FF* values reported to date compared with previously reported phenazine copolymeric derivatives in BHJ-PSCs. This work suggested that random conjugated terpolymers could be promising donor materials for application in PSCs.

**Acknowledgements**

This work was supported by the Major Program for cultivation of the National Natural Science Foundation of China (91233112), the National Natural Science Foundation of China (51273168, 21172187 and 21202139), the Ministry of Science and Technology of China (2010DFA52310), the Innovation Group and Xiangtan Joint Project of Hunan Natural Science Foundation (12JJ7002 and 12JJ8001), the key project of Hunan Provincial Education Department (13A102, 12B123), and the Postgraduate Science Foundation for Innovation in Hunan Province (CX2012B249, CX2013B268).

**Notes and references**

1. Y. F. Li, *Acc. Chem. Res.*, 2012, **45**, 723.
2. K. R. Graham, C. Cabanetos, J. P. Jahnke, M. N. Idso, A. E. Labban, G. O. N. Ndjawa, T. Heumueller, K. Vandewal, A. Salleo, B. F. Chmelka, A. Amassian, P. M. Beaujuge and M. D. McGehee, *J. Am. Chem. Soc.*, 2014, **136**, 9608.
3. P. Bujak, I. K. Bajer, M. Zagorska, V. Maurel, I. Wielgus and A. Pron, *Chem. Soc. Rev.*, 2013, **42**, 8895.
4. J. X. Wang, M. J. Xiao, W. C. Chen, M. Qiu, Z. K. Du, W. G. Zhu, S. G. Wen, N. Wang and R. Q. Yang, *Macromolecules*, 2014, **47**, 7823.

5. C. H. Cui, W. Y. Wong and Y. F. Li, *Energy Environ. Sci.*, 2014, **7**, 2276.

6. D. F. Dang, W. C. Chen, R. Q. Yang, W. G. Zhu, W. Mammod and E. G. Wang, *Chem. Commun.*, 2013, **49**, 9335.

7. M. Wang, H. B. Wang, T. Yokoyama, X. F. Liu, Y. Huang, Y. Zhang, T. Q. Nguyen, S. Aramaki and G. C. Bazan, *J. Am. Chem. Soc.*, 2014, **136**, 12576.

8. W. Y. Su, Q. P. Fan, M. J. Xiao, J. H. Chen, P. Zhou, B. Liu, H. Tan, Y. Liu, R. Q. Yang and W. G. Zhu, *Macromol. Chem. Phys.*, 2014, **215**, 2075.

9. K. Li, Z. J. Li, K. Feng, X. P. Xu, L. Y. Wang and Q. Peng, *J. Am. Chem. Soc.*, 2013, **135**, 13549.

10. K. Wang, Y. Zhao, W. L. Tang, Z. G. Zhang, Q. Fu and Y. F. Li, *Org. Electron.*, 2014, **15**, 818.

11. Y. H. Liu, J. B. Zhao, Z. K. Li, C. Mu, W. Ma, H. W. Hu, K. Jiang, H. R. Lin, H. Ade and H. Yan, *Nat. Commun.*, 2014, **5**, 5293.

12. W. Y. Su, M. J. Xiao, Q. P. Fan, J. Zhong, J. H. Chen, D. F. Dang, J. W. Shi, W. J. Xiong, X. W. Duan, H. Tan, Y. Liu and W. G. Zhu, *Org. Electron.*, 2015, **17**, 129.

13. H. C. Chen, Y. H. Chen, C. C. Liu, Y. C. Chien, S. W. Chou and P. T. Chou, *Chem. Mater.*, 2012, **24**, 4766.

14. W. T. Li, S. Albrecht, L. Q. Yang, S. Roland, J. R. Tumbleston, T. McAfee, L. Yan, M. A. Kelly, H. Ade, D. Neher and W. You, *J. Am. Chem. Soc.*, 2014, **136**, 15566.

15. J. Warnan, C. Cabanetos, R.Bude, A. E. Labban, L. Li and P. M. Beaujuge, *Chem. Mater.*, 2014, **26**, 2829.

16. C. Cabanetos, A. E. Labban, J. A. Bartelt, J. D. Douglas, W. R. Mateker, J. M. J.

Fréchet, M. D. McGehee and P. M. Beaujuge, *J. Am. Chem. Soc.*, 2013, **135**, 4656.

17. T. L. Nguyen, H. Choi, S. J. Ko, M. A. Uddin, B. Walker, S. Yum, J. E. Jeong, M. H. Yun, T. J. Shin, S. Hwang, J. Y. Kim and H. Y. Woo, *Energy Environ. Sci.*, 2014, **7**, 3040.
18. J. H. Chen, Q. G. Liao, G. Ye, D. He, X. Y. Du, W. G. Zhu, J. H. Liao, Z. Xiao and L. M. Ding, *Macromol. Chem. Phys.*, 2013, **214**, 2054.
19. J. Warnan, A. E. Labban, C. Cabanetos, E. T. Hoke, P. K. Shukla, C. Risko, J. L. Brédas, M. D. McGehee and P. M. Beaujuge, *Chem. Mater.*, 2014, **26**, 2299.
20. H. Tan, J. T. Yu, Y. F. Wang, J. H. Chen, Q. Tao, Y. Liu, J. Huang and W. G. Zhu, *Org. Electron.*, 2013, **14**, 1510.
21. J. W. Jung, F. Liu, T. P. Russell and W. H. Jo, *Energy Environ. Sci.*, 2013, **6**, 3301.
22. J. M. Jiang, H. C. Chen, H. K. Lin, C. M. Yu, S. C. Lan, C. M. Liu and K. H. Wei, *Polym. Chem.*, 2013, **4**, 5321.
23. J. Li, K. H. Ong, P. Sonar, S. L. Lim, G. M. Ng, H. K. Wong, H. S. Tan and Z. K. Chen, *Polym. Chem.*, 2013, **4**, 804.
24. W. J. Sun, Z. F. Ma, D. F. Dang, W. G. Zhu, M. R. Andersson, F. L. Zhang and E. G. Wang, *J. Mater. Chem. A*, 2013, **1**, 11141.
25. M. Zhang, F. Wu, Z. C. Cao, T. P. Shen, H. J. Chen, X. L. Li and S. T. Tan, *Polym. Chem.*, 2014, **5**, 4054.
26. T. E. Kang, K. H. Kim and B. J. Kim, *J. Mater. Chem. A*, 2014, **2**, 15252.
27. P. Shen, H. J. Bin, L. Xiao and Y. F. Li, *Macromolecules*, 2013, **46**, 9575.
28. Y. S. Huang, M. Zhang, H. J. Chen, F. Wu, Z. C. Cao, L. J. Zhang and S. T. Tan, *J.*

*Mater. Chem. A*, 2014, **2**, 5218.

29. K. H. Hendriks, G. H. L. Heintges, V. S. Gevaerts, M. M. Wienk and R. A. J. Janssen, *Angew. Chem. Int. Ed.*, 2013, **52**, 8341.
30. Y. Zhang, J. Y. Zou, H. L. Yip, K. S. Chen, D. F. Zeigler, Y. Sun and A. K.Y. Jen, *Chem. Mater.*, 2011, **23**, 2289.
31. Q. P. Fan, Y. Liu, M. J. Xiao, H. Tan, Y. F. Wang, W. Y. Su, D. L. Yu, R. Q. Yang and W. G. Zhu, *Org. Electron.*, 2014, **15**, 3375.
32. S. Li, Z. C. He, J. Yu, S. A. Chen, A. S. Zhong, R. L. Tang, H. B. Wu, J. G. Qin and Z. Li, *J. Mater. Chem.*, 2012, **22**, 12523.
33. J. Zhang, W. Z. Cai, F. Huang, E. G. Wang, C. M. Zhong, S. J. Liu, M. Wang, C. H. Duan, T. B. Yang and Y. Cao, *Macromolecules*, 2011, **44**, 894.
34. L. Ye, S. Q. Zhang, W. C. Zhao, H. F. Yao and J. H. Hou, *Chem. Mater.*, 2014, **26**, 3603.
35. L. Ye, S. Q. Zhang, L. J. Huo, M. J. Zhang and J. H. Hou, *Acc. Chem. Res.*, 2014, **47**, 1595.
36. M. J. Zhang, Y. Gu, X. Guo, F. Liu, S. Q. Zhang, L. J. Huo, T.P. Russell and J. H. Hou, *Adv. Mater.*, 2013, **25**, 4944.
37. B. Liu, X. W. Chen, Y. H. He, Y. F. Li, X. J. Xu, L. Xiao, L. D. Li and Y. P. Zou, *J. Mater. Chem. A*, 2013, **1**, 570.
38. K. Mahmood, H. Lu, Z. P. Liu, C. B. Li, Z. Lu, X. Liu, T. Fang, Q. H. Peng, G. W. Li, L. Li and Z. S. Bo, *Polym. Chem.*, 2014, **5**, 5037.
39. W. Lee, G. H. Kim, S. J. Ko, S. Yum, S. H Wang, S. Cho, Y. H. Shin, J. Y. Kim

and H. Y. Woo, *Macromolecules*, 2014, **47**, 1604.

40. G. W. Li, C. Kang, X. Gong, J. C. Zhang, C. H. Li, Y. C. Chen, H. L. Dong, W. P. Hu, F. H. Li and Z. S. Bo, *Macromolecules*, 2014, **47**, 4645.
41. T. S. Qin, W. Zajaczkowski, W. Pisula, M. Baumgarten, M. Chen, M. Gao, G. Wilson, C. D. Easton, K. Müllen and S. E. Watkins, *J. Am. Chem. Soc.*, 2014, **136**, 6049.
42. P. C. Zhou, Z. G. Zhang, Y. F. Li, X. G. Chen and J. G. Qin, *Chem. Mater.*, 2014, **26**, 3495.
43. Y. Wang, F. Yang, Y. Liu, R. X. Peng, S. J. Chen and Z. Y. Ge, *Macromolecules*, 2013, **46**, 1368.
44. D. F. Dang, W. C. Chen, S. Himmelberger, Q. Tao, A. Lundin, R. Q. Yang, W. G. Zhu, A. Salleo, C. Müller and E. G. Wang, *Adv. Energy Mater.*, 2014, **4**, 1400680.
45. Q. P. Fan, Y. Liu, P. G. Yang, W. Y. Su, M. J. Xiao, J. H. Chen, M. Li, X. D. Wang, Y. F. Wang, H. Tan, R. Q. Yang and W. G. Zhu, *Org. Electron.*, 2015, **23**, 124.
46. M. Wang, X. W. Hu, P. Liu, W. Li, X. Gong, F. Huang and Y. Cao, *J. Am. Chem. Soc.*, 2011, **133**, 9638.

## Figures and Tables

**Scheme 1.** Chemical structures of the terpolymers.

**Scheme 2.** Synthetic routes of the terpolymers.

**Fig. 1.** TGA curves of the terpolymers.

**Fig. 2.** UV-Vis absorption spectra of the terpolymers in solution (a), in thin films (b), and in their blend films with $PC_{71}BM$ at optimized ratio (c).

**Fig. 3.** Cyclic voltammogram curves for the terpolymers.

**Fig. 4.** HOMO and LUMO distribution mode of terpolymers obtained using calculated at the B3LYP/6-31G* level.

**Fig. 5.** *J-V* curves of the optimized hole-only terpolymer/$PC_{71}BM$ devices.

**Fig. 6.** *J-V* curves of the terpolymer/$PC_{71}BM$-based PSCs at optimized conditions under illumination of AM 1.5G, 100 mW/cm$^2$.

**Fig. 7.** *EQE* curves of the terpolymer/$PC_{71}BM$-based devices.

**Fig. 8.** AFM height images of the terpolymer/$PC_{71}BM$ blend films under the optimized condition.

**Fig. 9.** XRD spectra of the terpolymers thin films.

**Table 1.** Molecular weight and thermal properties of the terpolymers.

**Table 2.** Optical and electrochemical properties of the terpolymers.

**Table 3.** Photovoltaic properties of the terpolymer/$PC_{71}BM$-based PSCs at optimized conditions under illumination of AM 1.5G, 100 mW/cm$^2$.

## Scheme 1

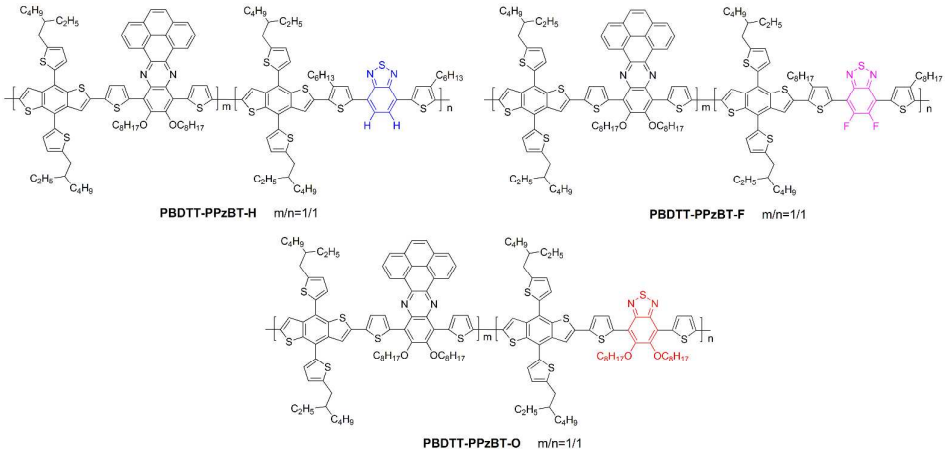


## Scheme 2

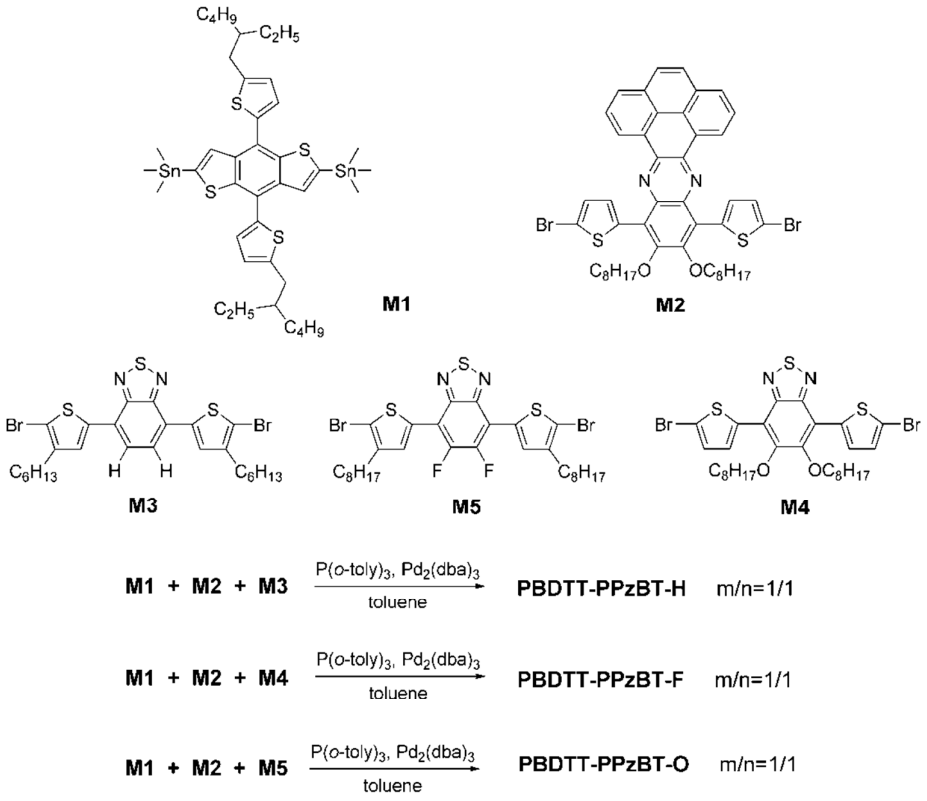

**Fig. 1**

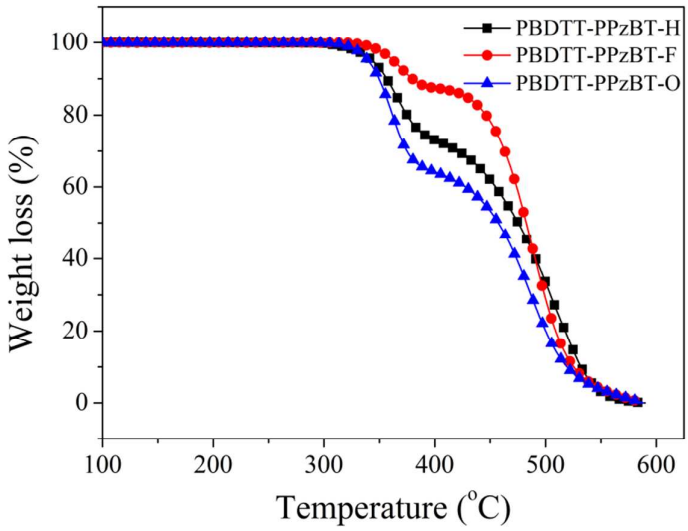


**Fig. 2**

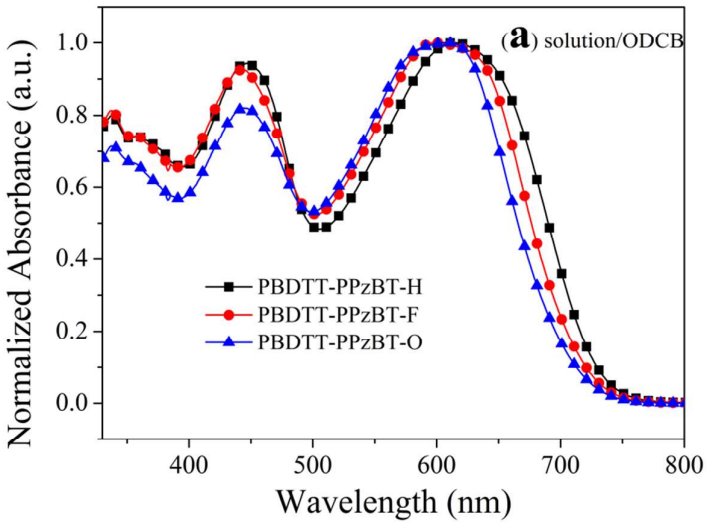

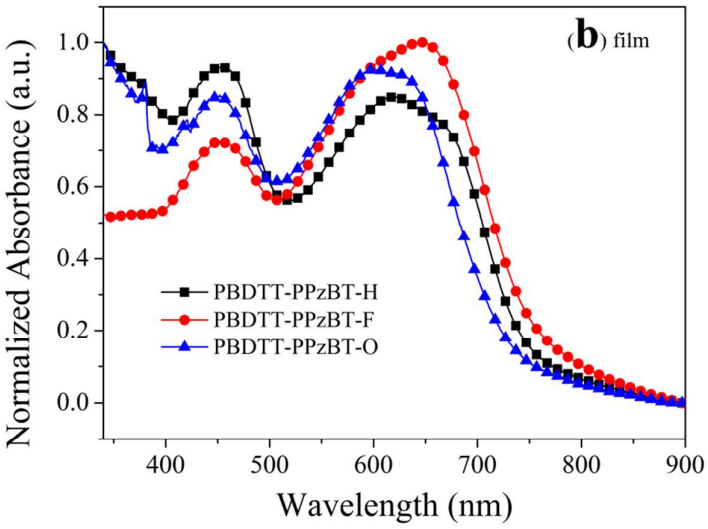


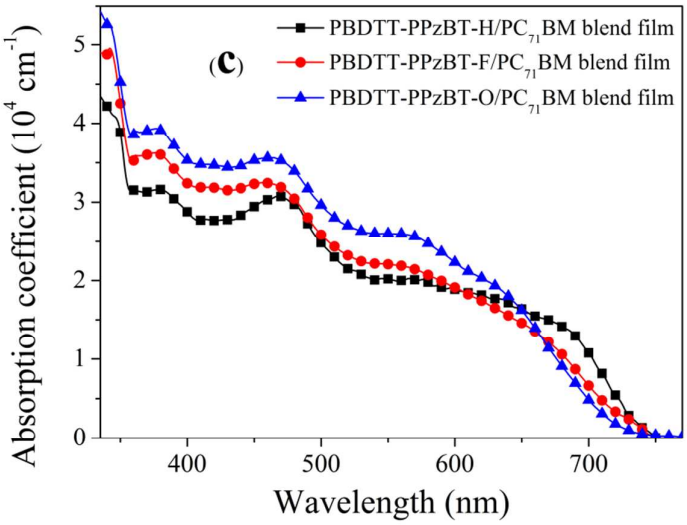

**Fig. 3**

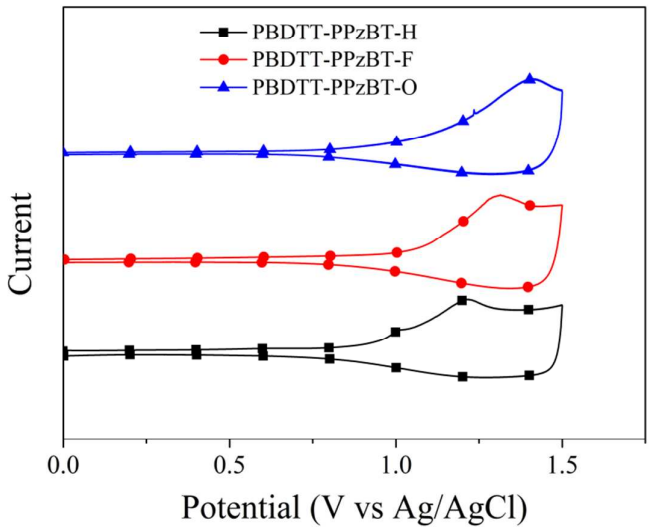


**Fig. 4**

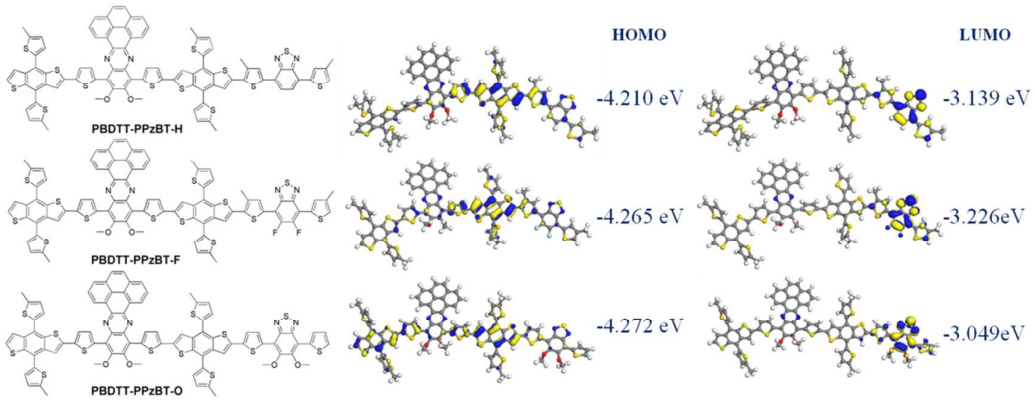

**Fig. 5**

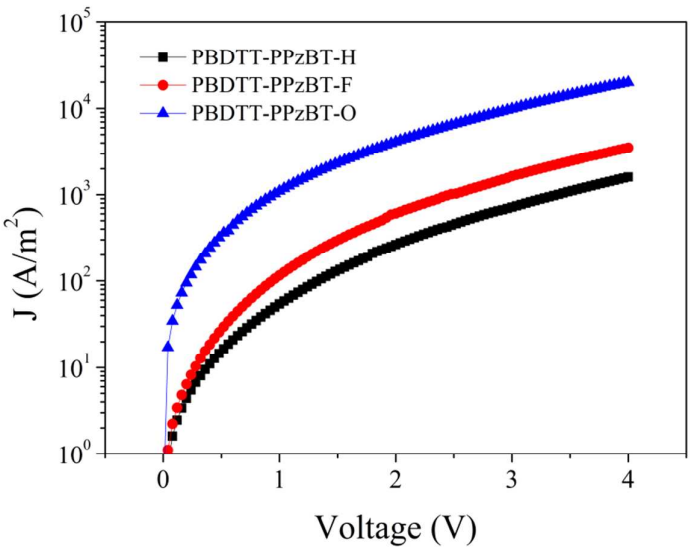


**Fig. 6**

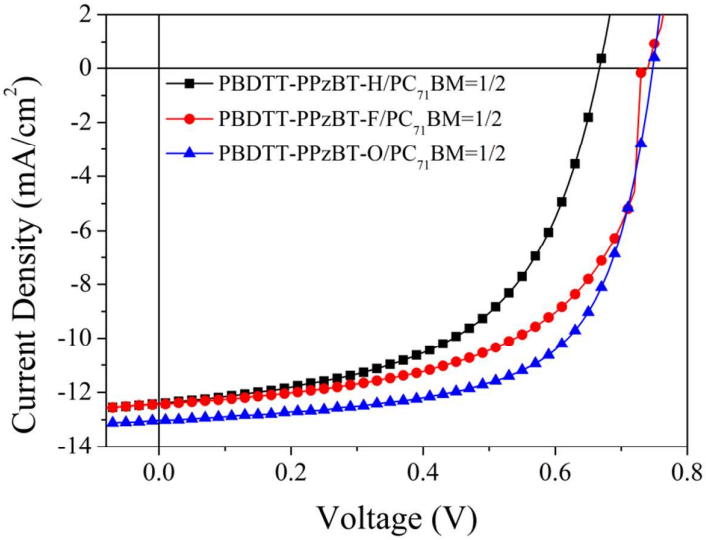

**Fig. 7**

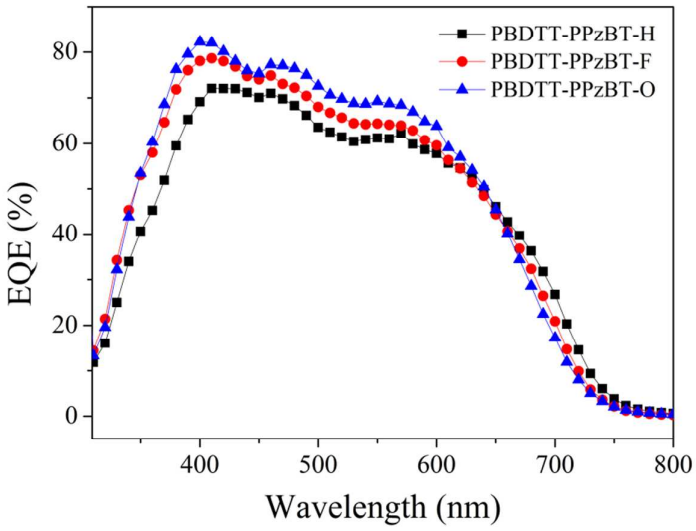


**Fig. 8**

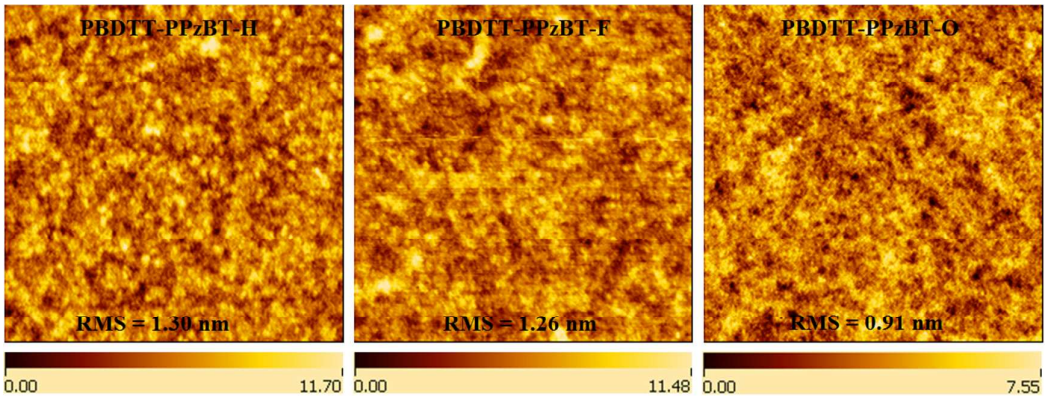

**Fig. 9**

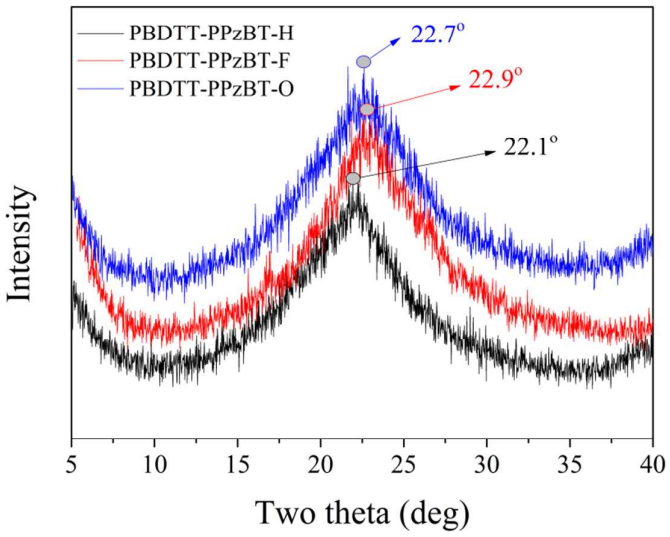

**Table 1**

| Terolymers | $M_n$ (kDa) | $M_w$ (kDa) | PDI | $T_d$ (ºC) |
|---|---|---|---|---|
| PBDTT-PPzBT-H | 29 | 90 | 3.10 | 350 |
| PBDTT-PPzBT-F | 45 | 110 | 2.24 | 363 |
| PBDTT-PPzBT-O | 52 | 131 | 2.52 | 341 |

**Table 2**

| Terpolymers | $\lambda_{abs}$ [a] /nm | $\lambda_{abs}$ [b] /nm | $\lambda_{onset}$ [b] /nm | $E_g^{opt}$ /eV | $E_{ox}$ /V | $E_{HOMO}$ /eV | $E_{LUMO}$ [c] /eV |
|---|---|---|---|---|---|---|---|
| PBDTT-PPzBT-H | 443, 617 | 453, 618, 658 | 771 | 1.61 | 0.80 | -5.15 | -3.54 |
| PBDTT-PPzBT-F | 443, 604 | 456, 602, 649 | 795 | 1.56 | 0.97 | -5.32 | -3.76 |
| PBDTT-PPzBT-O | 444, 611 | 449, 596, 626 | 759 | 1.63 | 0.95 | -5.30 | -3.67 |

[a] Measured in ODCB solution. [b] Measured in the neat film. [c] $E_{LUMO} = E_{HOMO} + E_g^{opt}$.

**Table 3**

| Polymer/$PC_{71}BM$ | $J_{sc}$/ mA $cm^{-2}$ | $V_{oc}$/ V | *FF*/ % | $PCE_{max}$/ % | Hole mobility/ $cm^2\ V^{-1}\ s^{-1}$ |
|---|---|---|---|---|---|
| PBDTT-PPzBT-H | 12.4 | 0.67 | 55.0 | 4.5 | $4.64\times10^{-5}$ |
| PBDTT-PPzBT-F | 12.5 | 0.74 | 59.6 | 5.5 | $8.61\times10^{-5}$ |
| PBDTT-PPzBT-O | 13.0 | 0.75 | 64.8 | 6.3 | $3.75\times10^{-4}$ |

# Graphical Abstract